BeBeC-2016-D4

TIME-DOMAIN IMAGING TECHNIQUES FOR AEROACOUSTIC SOURCES

J. Fischer, I. Rakotoarisoa, V. Valeau, D. Marx, C. Prax, and L.E. Brizzi
Institut PPRIME, CNRS-Université de Poitiers-ENSMA
Bât. B17 - 6, rue Marcel Doré - TSA 41105
86073 Poitiers Cedex 9 - France
Email: vincent.valeau@univ-poitiers.fr

Abstract

This study investigates the possibility of using far-field array processing methods for identifying aeroacoustic sources in the time domain. Two techniques are used in this purpose: the classical delay-and-sum beamforming technique, and the numerical time-reversal technique. The study shows the link between those approaches, together with their respective advantages. The use of such techniques is especially relevant for the analysis of non stationary and/or intermittent aeroacoustic sources. Some applications are presented for two case studies, including experimental data (forward facing step noise), and numerical data (jet noise). The study shows how the array processing techniques can be applied to evaluate the intermittent nature of aeroacoustic sources, and how short duration noisy events can be located both in the time and space domains.

1 INTRODUCTION

The beamforming technique is a classical array processing tool for imaging and identifying aeroacoustic sources in flows [7]. This technique is most generally calculated in the frequency domain, and often relies on time averages, or at least on a short-term assumption of signal stationarity. Conversely, in this paper, the array data is processed in the domain. The interest of such an approach is the study of the intermittent or non stationary character of the noise sources. Some recent studies showed, indeed, the intermittent nature of aeroacoustic sources, in particular for what concerns jet noise [5, 11]. The general idea is that the far field radiation of aeroacoustic sources is mostly due to a set of acoustic events of short duration (the intermittet events) that radiate sound efficiently.

Studying such property with an array processing method implies that the intermittent sources should be localized in space, but also in the time domain. Compared to previous studies focusing on source intermittency, the main contribution of the present study is to propose a localisation of the intermittent events both in the time and in the space domains by using array data, while past studies were only focused on the identification in the time domain, based on the far-field measurement at a single point.

In a first part (Sect. 2), a general presentation of time-domain imaging methods is proposed, based on the recent works of the same authors [18]. Two ways of performing the source detection are possible and will be presented: the first one is the classical time-domain delay-and-sum beamforming method, while the second one is the numerical time-reversal method. The respective advantages and application domains of those methods will be discussed. In the rest of the paper, the time-domain methods are applied to two case studies. In Sect. 3, a first application case is presented, focusing on the radiation of a forward-facing step in a flow, based on array measurements in an anechoic wind-tunnel. The second application case is presented in Sect. 4: it concerns the radiation of a turbulent jet, based on data obtained from a large eddy simulation. In both cases, some results will be provided concerning the intermittent events identified in the flow. The paper ends with a set of conclusive remarks.

2 TIME-DOMAIN IMAGING METHODS FOR AEROACOUSTICS

2.1 General formulation

Let us consider an array of M microphones measuring the far field noise at positions $\mathbf{r}_m$ $(1 \leq m \leq M)$, with $p(\mathbf{r}_m, t)$ being their output signals. The Green function of the propagation equation is noted down $G(\mathbf{r}, \mathbf{r_s}, t, \mathbf{U})$, $\mathbf{r}$ being the receiving position, and $\mathbf{r_s}$ the source position. The term $\mathbf{U}$ is the mean flow field, indicating the dependence of the propagation phenomena to the flow configuration. In this paper, two methods are used for identifying the source of sound within the flow: the classical delay-and-sum beamforming method (called BF method in the following), and a method based on the time-reversal principle. In a recent publication [18], it was shown that by using these two methods, the time-domain array output $z(\mathbf{r}, t)$ focused on a given position $\mathbf{r}$ can be written according to:

$$z(\mathbf{r}, t) \quad = \quad \sum_{m=1}^{M} p(\mathbf{r}_m, -t) *_t G(\mathbf{r}, \mathbf{r_m}, t, -\mathbf{U}), \tag{1}$$

so that the algorithm basically performs the sum of the convolution products in the time domain (denoted by the symbol $*_t$) of the time-reversed signals measured by the array's microphones with the Green function in the propagation medium. The quantity $-\mathbf{U}$ in the Green function argument states that in order to properly reverse the effects of the flow on propagation (refraction and convection), the direction of the flow should be inverted. In order to compute Eq. (1), two strategies are possible, as described below.

2.2 Delay-and-sum beamforming

The Green function can be written according to the following expression:

$$G(\mathbf{r}, \mathbf{r_s}, t, \mathbf{U}) = \frac{\delta(t - \Delta t_{(\mathbf{r_s},\mathbf{r})})}{\kappa(\mathbf{r_s}, \mathbf{r}) 4\pi |\mathbf{r_s} - \mathbf{r}|}, \tag{2}$$

$\Delta t_{(\mathbf{r_s},\mathbf{r})}$ being the propagation time of the sound wave from position $\mathbf{r_s}$ to position $\mathbf{r}$ and the term being $\kappa(\mathbf{r_s}, \mathbf{r})$ being a correction factor (referenced to the standard geometrical decrease in a quiescent infinite medium), modelling the wave dispersion when propagating through shear flows. By using Eq. (2), the time-domain array output of Eq. (1) can be rewritten (after reversing the time variable, ie., $t \to -t$), so that the standard formulation of the time-domain delay-and-sum beamforming is obtained:

$$z(\mathbf{r}, t) = \frac{1}{M} \sum_{m=1}^{M} w(\mathbf{r}, \mathbf{r_m}) p(\mathbf{r_m}, t + \Delta t_{(\mathbf{r},\mathbf{r_m})}), \tag{3}$$

$w(\mathbf{r}, \mathbf{r_m})$ being a weight function.

The main issue in computing Eq. (3) is the calculation of the retarded time, $\Delta t_{(\mathbf{r},\mathbf{r_m})}$. Its mathematical expression is only known for a uniform flow, but for a shear flow, some simplified analytical models can be used. In particular, the model developed initially by Amiet [1], based on an infinitely thin shear layer, is widely used in wind-tunnel applications, where the shear layer separates a uniform flow from a quiescent medium. For this configuration, another option, efficient at low Mach numbers, is to assume a propagation in a quiescent medium (not taking into account the flow effects on propagation), so that the obtained image is shifted downstream. It can be shown that this apparent spatial shift is equal to $\gamma \simeq \mathcal{M}H$, $\mathcal{M}$ and H being, respectively, the Mach number and the mean flow thickness. The obtained beamforming function $z(\mathbf{r}, t)$ then needs to be shifted properly upstream, ie., by plotting the function $z(\mathbf{r} - \gamma(\mathbf{U}/|\mathbf{U}|)), t)$ in order to recover the actual source position [14].

A more complicated solution, for calculating the retarded time $\Delta t_{(\mathbf{r_s},\mathbf{r})}$, is to use a ray-tracing algorithm [7, 19]. Compared to the last models, the ray-tracing model is more flexible as it can deal with arbitrary flow profiles. However, it suffers from a much higher algorithmic complexity, and can dramatically increase the calculation time. Moreover, in the case of important velocity gradients (ie., high Mach number flow), the density of rays intercepted by the array can be low. For this reason, some complex interpolation procedures are required, especially in three dimensions. This point is illustrated for a wind-tunnel flow configuration in Fig. 1: an acoustic source is located at the origin of the coordinate system in a flow at Mach number $\mathcal{M}$= 0.9, and the shear layer is located at Y/b = 7,5, b being the shear layer thickness. The medium above Y/b = 7,5 is quiescent, and typically the microphone array is located in this region (out of the flow). One can see that in this case, although the density of rays traced form the source is important, the density of rays actually traversing the shear layer is very low due to strong refraction and reflection effects, which raises algorithmic issues for calculating the terms $\Delta t_{(\mathbf{r},\mathbf{r_m})}$ for an array located above the shear layer.

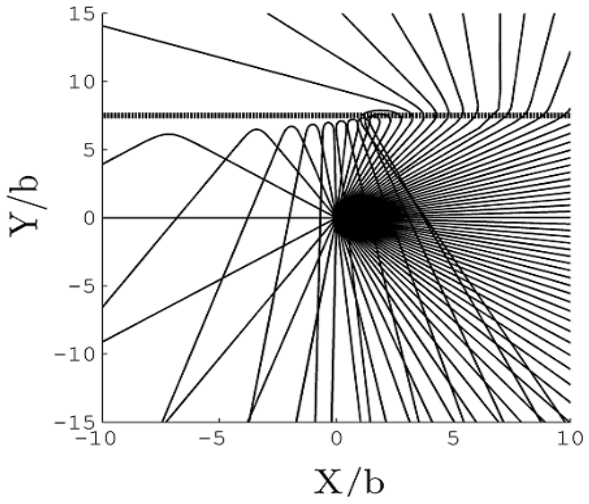

Figure 1: Ray-tracing modelling of the radiation of a harmonic source located at position (0;0) in a shear flow. The shear layer of thickness b is located at Y/b=7.5; the Mach number is $\mathcal{M}$= 0.9 below the shear layer, and the fluid is quiescent above the shear layer.

2.3 Numerical time-reversal

The second strategy for computing Eq. (1) is to solve numerically the propagation of the waves through the flow field. In this case, the method is equivalent to a source detection method based on the time-reversal (TR) principle [8]. The application of the TR principle to aeroacoustic source identification has been first proposed by Deneuve et al. [6] for numerical data; a few years later, an implementation of the TR principle was proposed by Padois et al. [15] for the analysis of experimental data. In this case, the wave propagation through the flow is modeled by using a code solving the Linearized Euler Equations (LEE) [2, 16]. This method has been further developed for experimental applications by Mimani et al., in particular for improving the resolution of the method [13].

The application of the TR method lies on two steps. First, a measurement of the far-field radiation of the aeroacoustic sources is carried out by using an acoustic array; the data can be taken from a numerical simulation or an experimental measurement. In a second step, the array data is time-reversed, as modeled by the $p(\mathbf{r}_m, -t)$ term in Eq. (1), so that the signals are played back in reversed order. The time-reversed data are then imposed as Dirichlet boundary conditions at the microphones locations, each microphone acting as a monopolar sound source. By application of the TR principle, the created sound field is back-propagated to the initial location of the source, on the condition that the flow effects are properly reversed, ie., the direction of the mean flow field is inverted. The generated sound field can then be viewed as the convolution product of the time-reversed data by the Green function describing the propagation in the reversed flow, as written in Eq. (1).

An example of application to two-dimensional numerical data is proposed in Fig. 2,

for a configuration identical to the one described in Fig. 1. The source is harmonic and located at $(0,0)$ in this example, and the far-field pressure field is recorded by a linear array located at Y/b=15. Fig. 1(a) presents a snapshot of the pressure field, displaying the significant convection, refraction and reflection effects that the wavefronts undergo, due to the strong mean velocity gradients. Fig. 1(b) displays a snapshot of the back-propagated field by using the time-reversed simulation, based on the linear array data. The quality of the wave focusing is poor as the array intercepts only a small part of the radiation. The beam passes through the source location at $(0;0)$ and continues its propagation as there is no dissipation at the source location. Some recent improvements aim at introducing a virtual «sink» at the source location in order to provide some dissipation, and improve the resolution [3, 12]. It is also observed that the quality of focusing is better in the direction X parallel to the array than in the direction Y perpendicular to the array, which is of common knowledge in array processing. For this reason, in the following, the time-domain array data of Eq. (1) will be investigated for positions $\mathbf{r}$ describing planes parallel to the array, in order to get the best resolution.

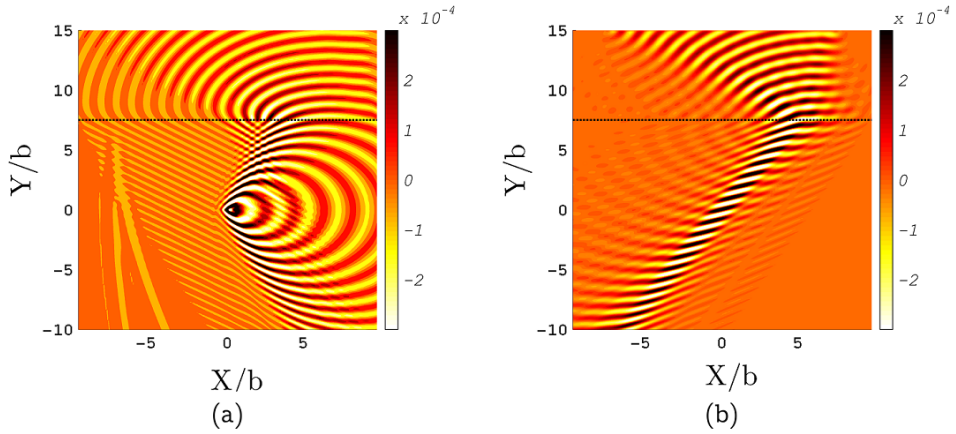

Figure 2: Snapshots of the pressure field generated by a harmonic source in the same configuration as the one in Fig. 1, modelled by solving the LEE equations. (a) measurement step, the linear array is located at Y/b=15 (the flow is oriented from the left to the right); (b) time-reversed simulation in the reversed flow field (from the right to the left).

2.4 Using the time-domain imaging function

In the case of a harmonic source, by definition stationary, it is possible to compute the Root Mean Square value of the distribution of the time-reversed pressure field; in this way, one can obtain a focal energetic spot which maximum is located at the source location. However, for such sources, the standard BF algorithm computed in the frequency domain will provide similar results, as pointed out by Padois et al. [15].

On the other hand, as mentioned in the introduction section, the time-domain imaging methods can provide some interesting views of aeroacoustic sources if the fluctuation or

the intermittency of the source is of interest. A method based on time-domain BF (or on the TR method) for the identification of short acoustic events in flows was proposed recently by Rakotoarisoa et al. [18]. It was shown that a short acoustic event (modeled by a pulse generated in the flow) produces a distinctive feature in an observation plane parallel to the array: a maximum is produced at the position where the pulse was emitted, and at a time corresponding to the emission time of the event. It is then possible to track very brief acoustic events emitted in the flow, and to identify both their emission time and position, which would not be achievable with the frequency domain BF; indeed, such a technique requires an important number of points (of the order of 100-1000) for calculating Fast Fourier Transforms (FFT), while the intermittent events in flows are very brief (their life time can be typically about a few signal samples).

An example is given in Figure 3 taken from Reference [18]. A bluff body with a three-dimensional shape representing a simplified car model is located in a wind-tunnel flow at speed 40 m/s. Some shedding phenomena on both sides of the body produce the so-called «A-pillar» vortices, which are known to be strongly non-stationary. Interacting with the sides of the model body, the A-pillar structure produces intermittent turbulent fluctuations that can radiate sound efficiently: the example of Figure 3 show some snapshots of the square of the time-domain BF technique (Eq. (3)) every 0.1 ms, calculated in a plane parallel to the array, and intersecting the model body (the array is planar, located above the model body and is designed according to the multi-arm spiral array, as designed by Underbrink [20]). The «focusing time» corresponds to the time at which a maximum is detected in the space-time domain, corresponding to the emission of a short aeroacoustic event. We can see that the emission location can be identified clearly on the left side of the body. The focusing time is immediately followed by diverging «wavefronts», which are in reality artifacts of the method and linked to the nature of the time-reversed pressure field [18]. Overall, if considered over a much larger time scale, the noise emitted appears to be wide-band in the frequency domain, but it is made of a great number of short events similar to the one in Fig. 3.

2.5 Beamforming or time-reversal?

The time-domain BF technique requires the Green function to be known analytically (which is the case for a uniform flow), or at least a simplified analytical model for the propagation through the flow (such as the Amiet's model for a wind-tunnel flow, see Section 2.2). If an exact expression of the Green function is available, then the time-domain BF technique gives results that are strictly identical to those given by the numerical time-reversal, as both methods basically rely on the same principle (Eq. (1)). The advantage of the BF technique is that is a cheap method in terms of computational cost. On the other hand, it is not useable for an arbitrary mean flow field, unless it is associated to a more sophisticated numerical model such as ray-tracing, but the computational cost then increases very substantially.

The numerical TR technique is definitely more demanding in terms of computational cost, as it requires a numerical simulation of the propagation. The convolution product of Eq. (1) is carried out by solving the time-reversed simulation of the waves through the flow. By principle, the simulated wave produces a beam focusing at the source location: it is said to be a «self-focusing» method. For this reason, it is very flexible in terms of

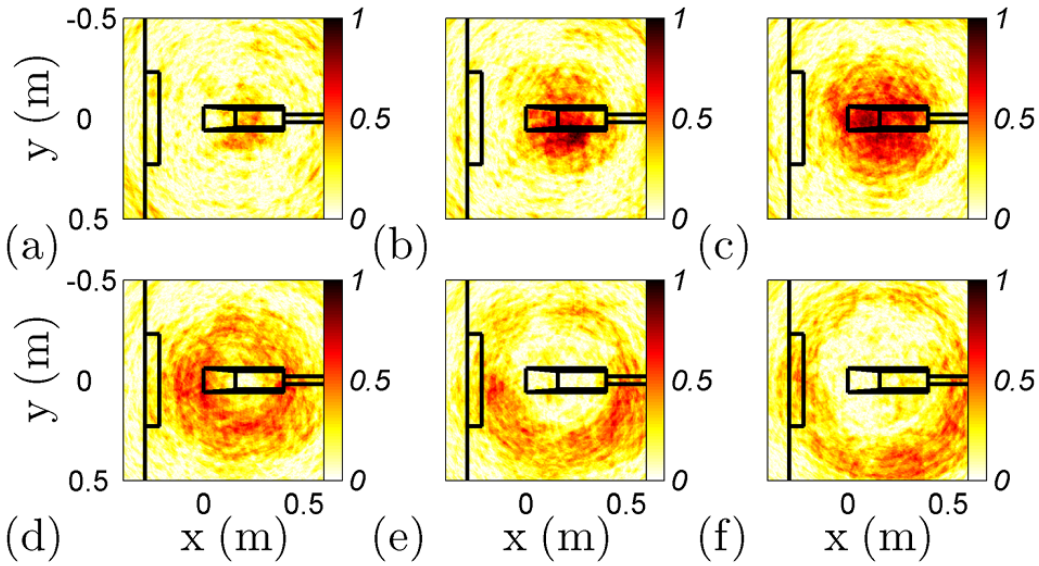

Figure 3: Example of an intermittent event on the left side of the model body, flow speed 40 m/s. Snapshots of square acoustic pressure calculated with time-domain BF technique (Eq. (3)) at (a) t_e - 0.1 ms, (b) t_e (focusing time), (c) t_e + 0.1 ms, (d) t_e + 0.2 ms, (e) t_e + 0.3 ms, and (f) t_e + 0.4 ms. The flow is oriented from the left to the right, and the black rectangle depicts the wind-tunnel nozzle exit. Taken from [18].

mean flow field, and, for example, some features can be taken into account in the propagation model such as: the shear layer thickness or thickening, the local wake produced by bodies in flow that could affect the propagation (struts for example)... Of course, such an accuracy in the model requires a preliminary measurement of the details of the flow field.

Another important advantage of the TR technique is its ability to model reflection and diffraction by rigid boundaries [21]. A great potential application of the technique is then the possibility of modelling such phenomena (eg., diffraction by struts, wind-tunnel nozzle or collector), in order to improve the source identification. From the time-reversed simulation, it is also possible to obtain an image of the source by frequency band, which would be equivalent to what is obtained with standard frequency-domain BF, with the advantage of taking into account the effects of walls or objects affecting the propagation. The respective advantages and drawbacks of the time-domain BF and numerical TR are summarised in Table 1.

Methods	Time-domain BF	Numerical TR
Advantages	Simple and cheap computation	Self-focusing
Drawbacks	Green function necessary	Numerical cost
Applications	Uniform or simple shear flow	Arbitrary flow field Rigid boundaries (diffraction, reflexion)

Table 1: Comparison of the time-domain BF and numerical TR techniques.

3 EXPERIMENTAL APPLICATION: INTERMITTENCY OF THE NOISE RADIATED BY A FORWARD-FACING STEP

In this section, we are interested by studying the intermittency of the noise radiated by a forward-facing step in a flow. This type of noise is known to be of broadband nature, and is a model for flow noise phenomena found in transport applications. The experimental setup is a bi-dimensional step located in a wind-tunnel flow; a general view of the experiment can be found in the picture of Fig. 4. The main characteristics of the open wind-tunnel are the following: the measuring test-section is 1.4 m long, and it is open in an anechoic room of cutoff frequency 300 Hz. The section of the upstream nozzle is (0.46×0.46) m^2, and the flow is bounded on its lower part by a flat wall with a forward-facing step of height 3 cm. The flow speed is 50 m/s ($\mathcal{M}$=0.15). The microphone array was designed according to a multi-arm spiral geometry [20]. There are five branchs of 6 phased microphones each (B&K model 4957). The array is parallel to the bottom plate, and located outside the flow. The acquisition system operates at a sampling frequency of 50 kHz. Further details about the experimental setup can be found in Ref. [9].

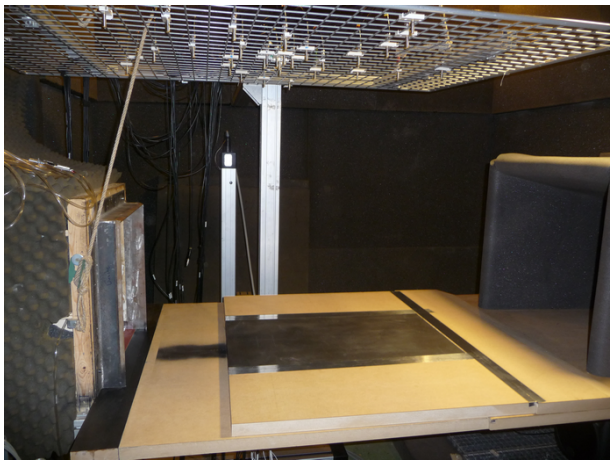

Figure 4: Picture of the test-section of the anechoic wind-tunnel, including the forward-facing step, the microphone array, and the nozzle and collector of the wind-tunnel.

The goal of the study is to extract, from the array data, a set of intermittent events that would be responsible for the main part of the energy of the radiated field. The intermittent

events are very brief acoustic events that should be identified both in terms of emission location and time. In the previous section, it was pointed out that, when using an imaging method such as BF or TR, the signature of a brief acoustic event is characterized by a maximum in space and time in the focusing plane. This focusing plane is chosen parallel to the array and intersecting the edge of the step (exactly, 3 cm above the bottom plane). A careful algorithm has then been designed, in order to track appropriate space-time maxima in the focusing plane, which details can be found in Ref. [9]. Basically, the detection is based on a one-dimensional signal $z_m(t)$, tracking the maxima in the focusing plane for each value of t. An important parameter is the threshold value for the detection of the maxima; the number of detected events appeared to be very sensitive to this threshold value.

First of all, some frequency-domain BF have been carried out, by using standard algorithms based on the calculation of the Cross-Spectrum matrix [7]. The cross-spectral terms of the matrix have been calculated by performing time averages according to the Welch's method (122 blocks of 4096 FFT points). The deconvolution technique DAMAS [4] was used to improve the resolution of the beamform maps. In Figure 5(d) and (e), some results are provided for two narrow frequency bands centered on 2 kHz and 5 kHz. The aeroacoustic broadband source is distributed along the span of the step, moving slightly with frequency. Overall, the results indicate that for frequencies in the range [1.5;3] kHz, the source radiates from slightly upstream the step (which might be due to the non stationary behaviour of the foot vortex upstream the step), while, for higher frequencies, it is more active downstream of the step (in the region where the flow detaches from the step).

The time-domain imaging method is now applied to the array data. In this study, the time-domain BF technique was preferred to the TR technique for its computational cheapness, and because, for the wind-tunnel flow, the simplified model of Amiet [1] is sufficient for a good estimation of the retarded times, as explained in Section 2.2. The algorithm for detecting the intermittent events was applied, and a catalogue of intermittent events was obtained, characterized by their emission times and locations, and their amplitudes. A cloud of intermittent events can then be obtained, showing their spatial distribution; it is represented in Fig. 5(a). As expected, the set of identified intermittent events is scattered along the edge of the step. Further statistical analysis showed that the emission times of the identified events follow a statistical Gamma law [9], which means that they are not governed by any deterministic mechanism. The mean width of the identified events was found to be of the order of 0.15 ms (ie., about 8 signal samples).

In order to be compared with the frequency-domain beamform maps at 2 and 5 kHz, the signals were preliminary processed with band-pass Finite Impulse Response filters in frequency bands [1.5;2.5] kHz and [4.5;5.5] kHz, and the time-domain BF was applied. The distribution results are presented in Figs. 5(b) and (c), respectively. The trend followed by the intermittent events is the following: the activity of the intermittent sources is higher in the region upstream the step in the frequency band [1.5;2.5] kHz, while the zone of activity moves upstream in the band [4.5;5.5] kHz. This behaviour is in agreement with the frequency-domain beamform maps of Figs. 5(d) (2 kHz) and (e) (5 kHz), respectively. This tend to validate the approach chosen for selecting the intermittent events creating the sound radiation, and for estimating their position. One can conclude that the classical

beamform maps used in aeracoustics, resulting of averaging processes, indicate a mean source of sound. The time-domain imaging approach allows the identication of the main events that have actually created the wide-band radiation. The approach is useful for bringing a complementary approach to aeroacoustics sources; the identification of the intermittent sources is a step towards a best understanding of the nature of broadband aeroacoustic sources.

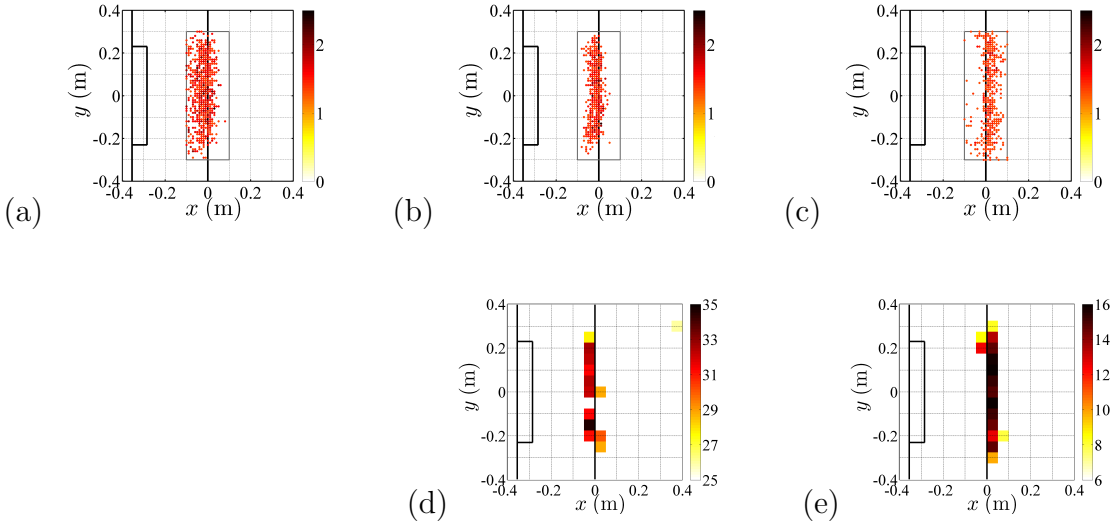

Figure 5: Forward facing step noise, $\mathcal{M} = 0,15$. Distribution of the intermittent sources detected by using the time-domain BF wihtout filtering the array signals (a), and after prior pass-band filtering the array signals in the range [1.5;2.5] kHz (b) et [4.5;5.5] kHz (c) (non-dimensionalized colorbar). Averaged narrow-band frequency-domain beamform maps at 2 kHz (d) and 5 kHz (e) (colorbar in dB ref. 2.10^{-5} Pa). The line at $x = 0$ represents the step, the left rectangle depicts the nozzle exit.

4 APPLICATION TO NUMERICAL DATA: THE RADIATION OF A TURBULENT JET

Recently, Rakotoarisoa et al. have used the TR method to estimate the source of sound in a simulated two-dimensional mixing layer at low Reynolds number [17]. The present work is an extension of this approach to a more turbulent and random flow: it is an attempt of localizing the intermittent sound sources in a jet, based on the database of a jet at Mach 0.9 and Reynolds 400000, obtained with a large eddy simulation (LES) of the Navier-Stokes equation (see Ref. [5]). Similarly to the approach described in the last section for the experimental step noise, the idea is to use the time-domain imaging method to localize the intermittent sources in the jet.

In the present case, the noise sources are located in regions with strong velocity gradients. There is no simple analytical model for taking into account propagation effects

in this case, so that the TR numerical method has been preferred for this study to the time-domain BF method. The general idea is to time-reverse the acoustic waves measured at the boundaries of the numerical domain and back-propagate the acoustic waves from the antenna towards the source. In this way the reconstructed sound field is not drowned in the flow field as it is the case for the LES data in the region close to the jet axis, where the sound field level is negligible compared to aerodynamic pressure fluctuations.

Using the same approach as in the last section, the goal is to detect the points where spatio-temporal maxima of the sound pressure occur, that are, points of the domain for which no spatial neighbour has a higher pressure level, either at, before, or after the considered time. Of course this is more legitimate for point sources than for extended sources that are difficult to deal with using this method. Finally, knowing the positions and instants of the maxima, it should be possible in principle to observe the flow fields at these same times and positions, and to educe the structures responsible for sound production. That is, it should be possible to make a conditional average of the flow field, where the condition is maximal sound field emission (a similar type of reasoning while with different tools has been used, for example, in Ref. [10]). This conditional average has not been conclusive though, at least because the database just contains 2000 snapshots, which is not sufficient to perform well-converged statistics or averages. Another post-processing method is thus considered as well below.

The LES database contains 2000 flow snapshots within a box of size $15D_j$ x $7D_j$ x $7D_j$ where D_j is the jet diameter. The trace of this box in the x-y plane is indicated by a red box in Fig. 6. The pressure and velocity on the faces of this box are used as inputs

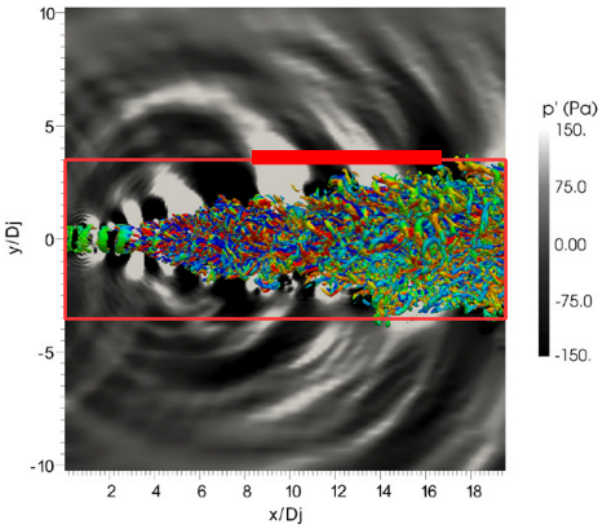

Figure 6: Snapshot of the LES database. Vortical structures in the jet in the x-y plane, together with their radiated sound field. Data produced with the LES are stored within the red box. The thick red line indicates the trace of the antenna in the x-y plane.

for the time reversal method. These data are at a distance of about 3.5 D_j from the jet axis. This is not in the acoustic far field for the lowest frequencies and there is a chance

that the data at low frequency are spoiled by non-acoustic near-field fluctuations. Since we are interested in the sound radiation from the coherent structures, known to occur at a Strouhal number of about $S_t \sim 0.2$, the acoustic pressure and velocity used for the time reversal method are high-pass filtered so that only the frequencies corresponding to a Strouhal number in the range $0.15 < St < 0.5$ are retained. The data on the boundaries of the domain after this filtering has been applied to the data saved in the acoustic far field outside of the domain; it has been checked that the filtered data used for the time reversal method correspond to acoustic fluctuations, and are free from near field disturbances. Moreover, the broadband character of the signal, obtained by keeping a frequency range rather than a particular frequency, allows this signal to be possibly intermittent, thus allowing for intermittent source detection.

Only a part of the data on the boundaries of the computational domain are used. Indeed the sound field created by the jet coherent structures is directive and is found at angles between 15 and 30 degrees from the jet outlet axis. The acoustic field used for the time reversal process is thus the one found within this angular sector. More specifically, the three-dimensional antenna is shown in Fig. 7 and its trace in the x-y plane is indicated by a thick line in Fig. 6. In Fig. 7 the jet exit is located

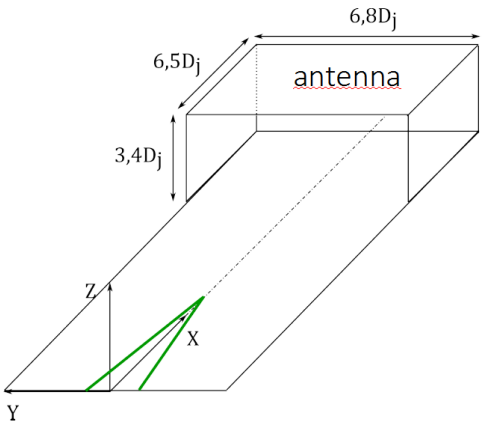

Figure 7: Antenna intercepting the directive noise of the jet.

in the x =0 plane with a flow velocity in the positive x-direction, and the triangle represents the footprint of the potential core in the $x-y$ plane. The antenna is continuous in the sense that it is made of all the grid points available in the numerical simulation.

The acoustic data recorded on the antenna are time-reversed and the back-propagation toward the source is obtained by a numerical solution of the LEE. The mean velocity upon which the sound travels is computed by averaging the flow fields of the LES and is shown in Fig. 8. As explained in Sect. 2.3, the direction of the mean flow needs also to be reversed, since both the transformations $t \to -t$ and $U \to -U$ are needed to warrant an invariance of the equations. Using the mean flow, the details of the acoustic/turbulence interaction are lost, but the refraction and convection of the wave by the mean flow is accounted for. The method takes into accurately account these effects and no analytic

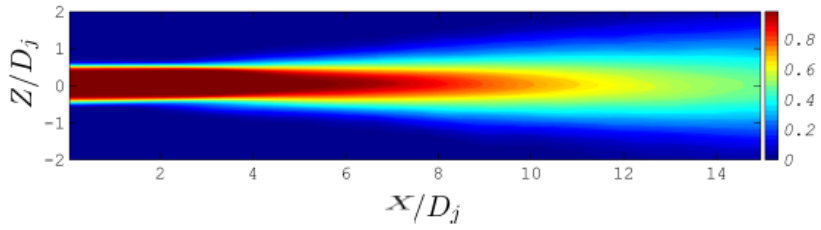

Figure 8: Mean flow calculated using the LES and used (after sign-reversal) as a base flow for the linearized Euler equations during the time-reversal stage.

model is required, which has been identified earlier as an advantage of the method.

Figure 9 (left part) shows the flow field and the acoustic field corresponding to some snapshot in the LES database. The corresponding acoustic field obtained by back

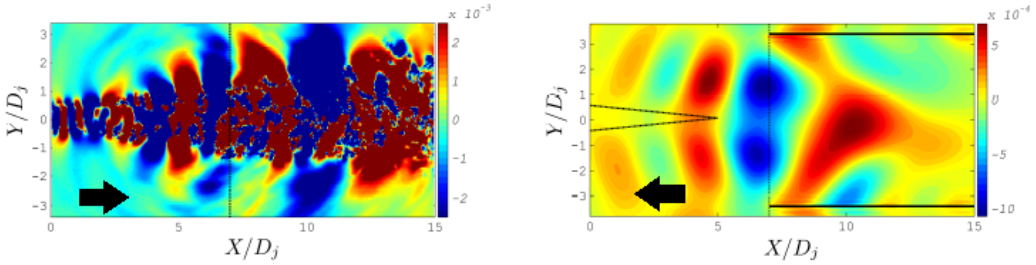

Figure 9: Left: flow and acoustic field obtained at some time during the LES simulation. Right: acoustic field reconstructed by time reversal using the LEE, at the same time. The arrows indicate the direction of the mean flow: toward $x > 0$ for the forward simulation; toward $x < 0$ for the time reversed simulation.

propagating the signal from the antenna (hereafter called reversed field) is also shown (right part). The plane in which the results are shown is parallel to the main part of the antenna (the two thick lines represent the trace of the antenna in the x-y plane), this is the plane where the resolution is maximal. The first thing to note is that the reversed field is free from the aerodynamic flow field. In the jet numerical simulation the vorticity field goes out of the domain through the right boundary (see Fig. 6), it is not intercepted by the antenna, and it is therefore not time reversed. Some acoustic wave fronts are visible in the reversed field which travels toward the $x < 0$ direction. The reversed field converges roughly toward the end of the potential core. This convergence is followed by a divergence in the region $x < 5$ since there is no sink to absorb the wave. Some spatial maxima in the reversed field are observed. By tracking these spatial maxima until the time when they are maximal in time, the spatio-temporal maxima are detected. Ideally, a three-dimensional detection should be performed, but presently a simpler two-dimensional detection is used and performed in the x-y plane shown in Fig. 9. Based on some tests made on known sources (pressure pulses with known positions and emission time sent in the same mean flow as that of the jet), the time precision for the spatio temporal detection is about $0.16 D_j/U_c$ where $U_c = 0.6 U_j$ is the convection speed

of structures (U_j is the jet speed).

The resulting spatio-temporal maxima obtained in the x-y plane are shown in Fig. 10. The colormap in this figure represents the overall pressure level calculated over the whole duration of the time-reversed simulation, and the symbols are individual maxima occuring at intermittent instants. These maxima are located on each side of the end of the potential core. As mentioned above, the initial objective of the study was to isolate a

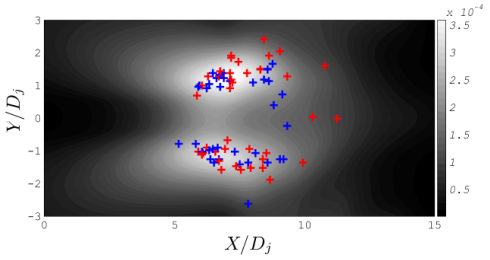

Figure 10: Root mean square pressure obtained during the time-reversed simulation, given in shades of gray. Symbols are the individual spatio-temporal maxima.

set of maxima clustered around some spatial domain, then to consider the flow fields at the instants corresponding to these maxima, and to average these flow fields to obtain an averaged flow field containing a sound emission feature. However, the database does not contain a sufficiently large number of instants and this objective has not been reached and we have turned to the method explained thereafter. Visual inspection of the flow field seems however to indicate that the maxima of acoustic emission are linked to an axisymmetric pressure wave in the jet.

Another attempt has been made to determine whether the spatio-temporal maxima of the reversed acoustic field (assumed to correspond to a source) can be connected to the flow field. An azimuthal Fourier mode decomposition of the acoustic far field (at r=6D_j) shows that this field is dominated by the axisymmetric mode. Since it is reasonable to infer that an axisymmetric acoustic mode in the far field may be generated by an axisymmetric aerodynamic mode in the near field, an azimuthal mode decomposition of the near pressure field has been done has well. This decomposition was carried out at axial position x=6D_j and radius r=0.5D_j. The resulting amplitude for the axisymmetric mode of aerodynamic pressure is shown in Fig. 11. This amplitude possesses some spikes and the more significant ones (ie, those having an amplitude larger than some given threshold) are detected. The time lag τ between the spatio-temporal maxima in the reversed acoustic field and the spikes of the aerodynamic pressure in the direct database is then computed. Figure 12 provides an histogram of this lag. On average, the lag is 0, which shows that sound emission as detected by time reversal happens at the same time as the near field pressure axisymmetric mode in the vicinity of the end of the potential core. Visual inspection of the aerodynamic pressure fields tend to show that actually the pressure axisymmetric mode is a pressure wave that is not necessarily localized at the end of the potential core but rather is spread over a large streamwise extent.

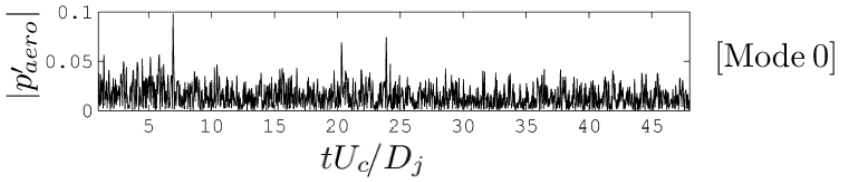

Figure 11: Amplitude of the axisymmetric azimuthal mode (order 0) of aerodynamic pressure (calculated from the history of the flow fields in the LES database), calculated at x=6D_j and r=0.5D_j.

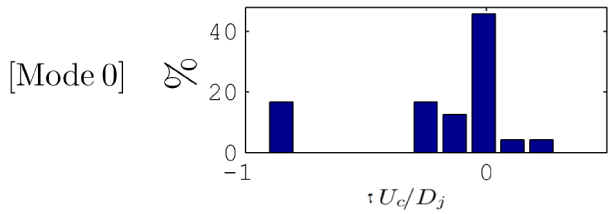

Figure 12: Histogram of the time lag between the instants corresponding to spatio-temporal maxima in the time-reversed acoustic field and the instants corresponding to the spikes of the aerodynamic pressure in the LES database.

To conclude, in spite of some approximations in the method (in particular, a pointwise detection of spatio-temporal acoustic maxima is made in a 2D plane), these preliminary results tend to show that it is possible to relate sound emission and the flow field in three-dimensional flows by using a time-reversal method.

5 Conclusions

In this study, two array processing techniques working in the time domain: the time-domain delay-and-sum BF, and the numerical TR technique, are used for the identification of the intermittency of aeroacoustic sources. The time-domain BF technique is computationally cheap, but requires the knowledge of the Green function of the propagation equation; in aeroacoustics, this is achievable in simple cases (uniform flow, or shear flow with infinitely thin shear layer). On the other hand, the numerical TR technique is a self-focusing method requiring a simulation of the wave propagation, so that it is very flexible in terms of mean flow field, and can take into account the effect of rigid boundaries. Its drawback is that it requires a simulation of the wave propagation, so that its computational cost is much higher.

In order to identify the intermittent acoustic events in the flow, the array processing techniques are processed in order to obtain an image of the pressure in a focusing plane parallel the array. The sources are characterized by local maxima in the time and space domains, and some tracking techniques of those maxima are then applied.

Two applications are considered. The first one is taken from measurements in a wind-

tunnel, consisting in the measurement of the far field noise produced by a forward-facing step in a flow. A catalogue of intermittent events is obtained by using the time-domain BF, and the spatial distribution of the events appears to be in good agreement with the position of the source identified by using the popular frequency-domain BF technique. The second application is based on the large eddy simulation of a turbulent jet. The numerical TR technique is applied, and the events are localized at the end of the potential core of the jet. In spite of the limited lenght of the database, the emission of the events seem to be correlated with some peaks of the axisymmetric mode of thet jet. Some further investigations on the relationship between the emission of the acoustic events and some local fluid dynamics events should be carried out in the future.

References

[1] R. K. Amiet. "Refraction of sound by a shear layer." *J. Sound Vib.*, 58, 467–482, 1978.

[2] C. Bailly and D. Juvé. "Numerical solution of acoustic propagation problems using linearized euler equations." *AIAA Journal*, 38, 22–29, 2000.

[3] E. Bavu, C. Besnainou, V. Gibiat, J. de Rosny, and M. Fink. "Subwavelength sound focusing using a time-reversal acousic sink." *Acta Acustica United with Acustica*, 93, 706–715, 2007.

[4] T. Brooks and W. Humphreys. "A deconvolution approach for the mapping of acoustic sources (DAMAS) determined from phased microphone arrays." *J.Sound Vib.*, 294, 856–879, 2006.

[5] A. Cavalieri, G. Daviller, P. Comte, P. Jordan, G. Tadmor, and Y. Gervais. "Using large eddy simulation to explore sound-source mechanisms in jets." *J. Sound Vib.*, 330, 4098–4413, 2011.

[6] A. Deneuve, P. Druault, R. Marchiano, and P. Sagaut. "A coupled time-reversal/complex differentiation method for aeroacoustic sensivity analysis: towards a source detection procedure." *J. Fluid Mech.*, 642, 181–212, 2009.

[7] R. Dougherty. *Aeroacoustics Measurements*, chapter Beamforming In Acoustic Testing. Springer, Berlin, 2002.

[8] M. Fink. "Time-reversal acoustics." *Journal of Physics: Conference Series*, 118, 1–28, 2008.

[9] J. Fischer, V. Valeau, and L.-E. Brizzi. "Beamforming of aeroacoustic sources in the time domain." In *Internoise S014, Melbourne*. 2014.

[10] J. I. Hileman, B. S. Thurow, E. J. Caraballo, and M. Samimy. "Large-scale structure evolution and sound emission in high-speed jets : real-time visualization with simultaneous acoustic measurements." *J. Fluid Mech.*, 544, 277–307, 2005.

[11] M. Kearney-Fischer, A. Sinha, and M. Samimy. "Intermittent nature of subsonic jet noise." *AIAA Journal*, 51 (5), 1142–1155, 2013.

[12] A. Mimani, C. J. Doolan, and P. R. Medwell. "Enhancing the focal-resolution of aeroacoustic time-reversal using a point sponge-layer damping technique." *JASA Express Letters*, 136, 199–205, 2014.

[13] A. Mimani, D. Moreau, Z. Prime, and C. Doolan. "Enhanced focal-resolution of dipole sources using aeroacoustic time-reversal in a wind tunnel." *Mechanical Systems and Signal Processing*, 72-73, 925–937, 2016.

[14] T. Padois, C. Prax, and V. Valeau. "Numerical validation of shear flow corrections for beamforming acoustic source localisation in open wind-tunnels." *Applied Acoustics*, 74, 591–601, 2013.

[15] T. Padois, C. Prax, V. Valeau, and D. Marx. "Experimental localization of an acoustic sound source in a wind-tunnel flow by using a numerical time-reversal technique." *J. Acoust. Soc. Am.*, 132, 2397–2407, 2012.

[16] C. Prax, F. Golanski, and L. Nadal. "Control of the vorticity mode in the linearized euler equations for hybrid aeroacoustic prediction." *J. Comp. Phys.*, 227, 6044–6057, 2008.

[17] I. Rakotoarisoa, J. Fischer, D. Marx, V. Valeau, C. Prax, L.-E. Brizzi, and C. Nana. "Detection of non-stationary aeroacoustic sources by time-domain imaging methods." In *Proc. 20th AIAA/CEAS Aeroacoustics Conference*, 2916. 2014.

[18] I. Rakotoarisoa, J. Fischer, V. Valeau, D. Marx, C. Prax, and L.-E. Brizzi. "Time-domain delay-and-sum beamforming for time-reversal detection of intermittent acoustic sources in flows." *J. Acoust. Soc. Am.*, 136, 2675–2686, 2014. doi: 10.1121/1.4897402.

[19] H. Schwartz, C. Prax, J. Pineeau, J. Valière, and G. Feuillard. "Application of ultrasound for the estimation of flight velocity direction on an aircraft fuselage." *Applied Acoustics*, 90 (1), 171–180, 2015.

[20] J. Underbrink. *Aeroacoustics Measurements*, chapter Aeroacoustic Phased Array Testing in Low Speed Wind Tunnels. Springer, Berlin, 2002.

[21] E. Vergnault, O. Malaspinas, and P. Sagaut. "Noise source identification with the lattice Boltzmann method." *J. Acoust. Soc. Am.*, 133, 1293–1305, 2013.